

---

# Morphologic Studies on the Biologic Seal of Titanium Dental Implants. Report II. In Vivo Study on the Defending Mechanism of Epithelial Adhesion/Attachment Against Invasive Factors

Haruyuki Kawahara, DDS, PhD\*/Dai Kawahara, DDS, PhD\*\*/  
Yoshiaki Mimura, DDS, PhD\*\*\*/Yoichiro Takashima, MD, PhD\*\*\*\*/Joo L. Ong, PhD\*\*\*\*\*

---

Clinical measurements on gingival indices and morphologic observations were performed in this study to verify the defending mechanism of gingival soft tissue against foreign invasions from the perspective of epithelial adhesion/attachment to implant surfaces in the monkey mandible. The following zones were observed using scanning electron microscopy: (1) plaque zone, suggesting susceptibility of the gingival tissue to bacterial invasion; (2) nude zone, demonstrating indirect adhesion of epithelial cells to the implant surface through the mucous layer and preventing bacterial invasion; and (3) epithelial cell attached zone, having greater bond strength of epithelial cells at the cell-implant interface as compared to cell-cell bonding within the epithelial cell layer. This study suggested that epithelial cell attachment/adhesion may play a dominant role in retaining the successful condition of a dental implant.

(INT J ORAL MAXILLOFAC IMPLANTS 1998;13:465-473)

**Key words:** biologic seal, cell adhesion, gingival index, implant, scanning electron microscopy

---

Biocompatibility and bioadhesiveness at the implant-tissue interface are critical in establishing a successful dental implant. Many investigations have focused on the osseointegration of bone tissue adhesion/ankylosis to dental implants. However, few studies have investigated the biologic seal of soft tissue adhesion/attachment to the abutment post of the implant. Because the biologic seal is considered a

dominant factor in the success of dental implants, light and electron microscopy analyses were performed in this study to verify the actual state of gingival soft tissue adhesion to the abutment post in vivo.

## Materials and Methods

The implants used in this study were blade-type polycapillary titanium implants (PCI)<sup>1</sup> (Toho-Titanium, Chigasaki, Kanagawa, Japan) that have been approved for clinical use in Japan. These implants are made of commercially pure titanium (JIS, TP-35) and are of a size suitable for the mandible of a Japanese monkey. The abutment post was polished to a mirror-like surface ( $R_z = 0.5 \mu\text{m}$ ), and the implants were cleaned with acetone and sterilized using ultraviolet irradiation (Fig 1).<sup>1-3</sup> The blade-type abutment post was selected for this study because of its ease for scanning electron microscopic (SEM) investigations.

Institutional Review Board's approval for the use of monkeys in this study was obtained prior to the beginning of the experiment. Appropriate consideration was given to the policies, standards, and guidelines for the proper use, care, handling, and treatment of ani-

---

\*President and Professor, Institute of Clinical Materials, Osaka, Japan.

\*\*Head of Research Section, Institute of Clinical Materials, Osaka, Japan.

\*\*\*Head of Clinical Research Section, Institute of Clinical Materials, Osaka, Japan.

\*\*\*\*Professor and Chairman, Department of Anatomy, Ehime University School of Medicine, Shigenobu, Japan.

\*\*\*\*\*Assistant Professor, University of Texas Health Science Center at San Antonio, Department of Restorative Dentistry, Division of Biomaterials, San Antonio, Texas.

**Reprint requests:** Dr Joo L. Ong, Department of Restorative Dentistry, Division of Biomaterials, University of Texas Health Science Center at San Antonio, 7703 Floyd Curl Drive, San Antonio, Texas 78284-7890.

**Table 1** Clinical Investigations of Gingival Tissue Responses to the Successful Implants

Clinical measures*	No. weeks postimplantation			
	4	12	24	36
Plaque Index (%)	10	20	80	80
Bleeding Index (%)	10	30	20	20
Probing depth (mm $\pm$ SD)	3.08 $\pm$ 1.61	2.50 $\pm$ 1.43	1.56 $\pm$ 1.29	1.56 $\pm$ 1.40
Periotron value ( $\pm$ SD)	6.50 $\pm$ 3.89	5.30 $\pm$ 3.00	4.10 $\pm$ 2.08	3.10 $\pm$ 1.66
Mobility value ( $\pm$ SD)	2.61 $\pm$ 0.67	1.15 $\pm$ 0.34	1.32 $\pm$ 0.47	1.06 $\pm$ 0.45

\*All values were measured on the lingual and buccal sides of each implant.

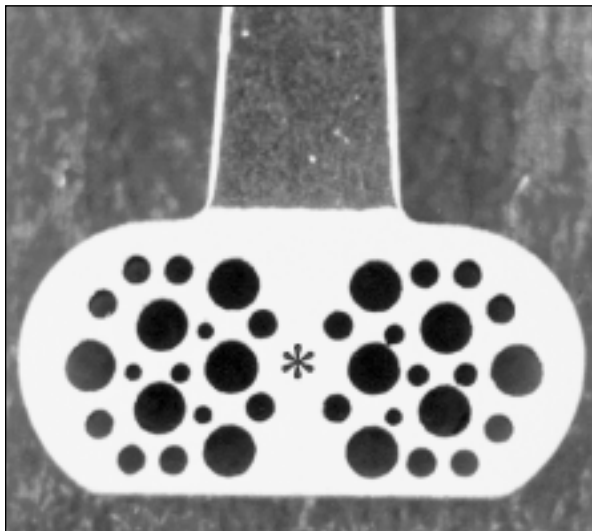


**Fig 1** Titanium polycapillary implant placed in monkey mandible. The abutment post on the implant has a mirror-like surface, and the implant body (asterisk) is roughened by means of a 4% hydrofluoric pickling acid solution.

mals. Six months after the extraction of the first molar from each side of the monkey's mandible, one implant was placed on each side. A total of six implants were used in three monkeys. At 12 weeks after placement, the superstructure of a single metal crown (type III gold-palladium-silver alloy) was mounted.

Single-blinded clinical evaluations of gingival tissue responses to the titanium implants were performed by: (1) measuring the Gingival Indices of probing depth (PD) with a modified Community Periodontal Index of Treatment Needs (CPITN) probe<sup>4</sup> using less than 0.2 N probing force<sup>4</sup>; (2) measuring the Bleeding Index (BI) using the BI method; (3) measuring the Plaque Index (PI) with a percentage of the stained surfaces using 2% fuchsin solution; (4) measuring the Periotron value (PV) (Ora Flow, Amityville, NY)<sup>5</sup>; and (5) measuring the mobility value (MV) of the implants using the Mobility Checker (Toei Electric, Kawasaki, Kanagawa,

Japan).<sup>6</sup> The results were statistically compared using the analysis of variance (ANOVA). The alpha level for data analysis was set at  $\alpha = 0.05$ , and differences were considered significant if  $P < .05$ .

After finishing all clinical investigations at 36 weeks postimplantation, the monkeys were sacrificed under barbitol anesthesia by perfusing 3% glutaraldehyde solution regulated with 0.2 mol/L cacodylate buffer in pH 7.4 into the carotid artery. The mandibles were sectioned into small blocks that included the implant and adjacent gingival tissue after the superstructure was removed.

The block was cut into two pieces with a diamond saw under frozen conditions. One block was analyzed under a light microscope and the other using SEM. For SEM analyses, the gingival tissue was peeled from the implant post surface and tied with pins. The block specimen was refixed with 3% glutaraldehyde solution for 24 hours. The geographic distribution of bacterial flora and epithelial cell attachment/adhesion were evaluated at the subgingival area of the post surface.

## Results

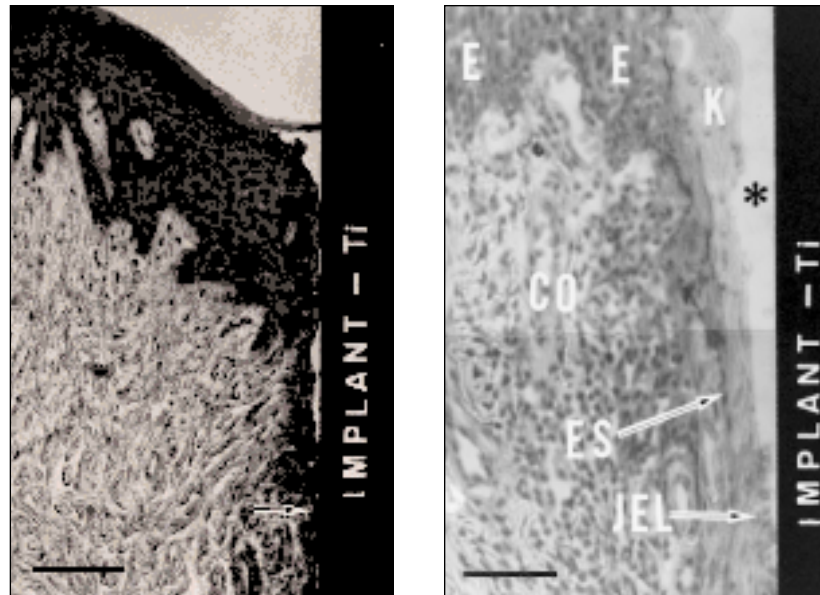
**Clinical Investigations on Gingival Index.** At 12 weeks after the mounting of the superstructure (24 weeks postimplantation), one implant was described as unserviceable because of gingivitis and considerable mobility. The implant had an MV of 4.52, a PD of 12.5 mm, a BI of 100%, a PV of 60 or more, and a PI of 100%. This unsuccessful implant was not included in the statistical analysis of clinical measurements.

Normal range of the MV in a natural tooth is 0.5 to 2.5.<sup>5</sup> At 4 weeks postimplantation, the mean MV ( $\pm$  1 SD) for the five implants testing in buccal and lingual directions was  $2.61 \pm 0.67$  (Table 1). The MV significantly decreased to  $1.15 \pm 0.34$ ,  $1.32 \pm 0.47$ , and  $1.06 \pm 0.45$  at 12, 24, and 36 weeks postimplantation, respectively.

Table 1 also shows the PD and PV at 4, 12, 24, and 36 weeks postimplantation. At 4 and 12 weeks

**Fig 2** (Left) Gingival tissue contact to the successful implant 36 weeks postimplantation. Arrow indicates the cervical epithelialization. (Bar = 200  $\mu$ m.)

**Fig 3** (Right) Epithelial cell adhesion to the successful implant 36 weeks postimplantation. E = epithelium; CO = connective tissue; K = keratinized epithelium; ES = epithelial sheath; JEL = junctional epithelial-like cell; asterisk = gingival pocket. (Bar = 100  $\mu$ m.)



postimplantation (prior to the mounting of the superstructure), the mean PD ( $\pm$  1 SD) at the two sites of each implant post (buccal and lingual) was  $3.08 \pm 1.61$  mm and  $2.50 \pm 1.43$  mm, respectively. At 24 and 36 weeks (after the mounting of the superstructure), the mean PD ( $\pm$  1 SD) significantly decreased to  $1.56 \pm 1.29$  mm and  $1.56 \pm 1.40$  mm, respectively. As with the PD, a statistically higher PV was observed at 4 and 12 weeks postimplantation. The mean PV ( $\pm$  1 SD) at 4 and 12 weeks postimplantation (prior to the mounting of the superstructure) was  $6.50 \pm 3.89$  and  $5.30 \pm 3.00$ , respectively. However, at 24 and 36 weeks postimplantation, the mean PV ( $\pm$  1 SD) significantly decreased to  $4.10 \pm 2.08$  and  $3.10 \pm 1.66$ .

Also shown in Table 1, the BI ranged from 10 to 30% throughout the study. The PI was at a low level of 10 to 20% before the mounting of the superstructure. After the superstructure was mounted, at 24 weeks, the PI increased to 80%. Plaque of bacterial flora was observed using the SEM analyses on all surfaces of the six implants at 36 weeks postimplantation.

**Light Microscopic Observation.** The tooth neck was covered with gingival tissues and was protected from marginal contamination by the junctional epithelium that was attached closely to the tooth surface. The keratinized epithelium of the oral mucosa continued to the oral sulcular epithelium and grew downward between the junctional epithelium and the prickle cell layer to the root apex. Small changes in tissue response were observed at the titanium implant as compared to the natural tooth. The keratinized epithelial cells grew downward along the implant post surface to the implant apex. However, their cellular

characteristics gradually changed to a more nonkeratinized state and had a more vital condition in the deeper area, in which the keratinized cells transformed to a junctional epithelial-like cell (JELC). The flattened epithelial cell sheath followed the JELC (Figs 2 and 3). Apical growth of epithelialization was observed along the post surface. At the site of cervical epithelialization, advanced epithelial cells came into contact with the fibrous tissue adhered/attached to the implant post surface (Figs 2 and 3).

When pathologic symptoms were caused by mechanical and chemical irritation as a result of setting cement, plaque of bacterial flora, and debris invasion, the epithelial cells showed degeneration with swelling and karyorrhexis. As shown in Fig 4, the degeneration of epithelial cells was accompanied by an inflammatory reaction of round cell migration and/or infiltration into the epithelial tissue layer from the submucous connective tissue. Some of the epithelial cells were agitated by pathogenic factors, and the apical epithelialization developed actively along the implant surface and was restrained with a barrier of connective tissue attachment (Fig 5).

**SEM Investigation.** Figure 6 shows the surface of a serviceable implant post after the gingival tissue has been peeled off. From the SEM micrograph, three zones (plaque, nude, and epithelial cell attachment) were observed. The plaque zone (PZ) consisted of bacterial flora and debris, which were located in the area of the implant crevice. The nude zone (NZ), a mucous substance, consisting of a sandwich layer of extracellular substance and oral and body fluids, was observed in the area of indirect epithelial cell adhesion. The epithelial cell attach-

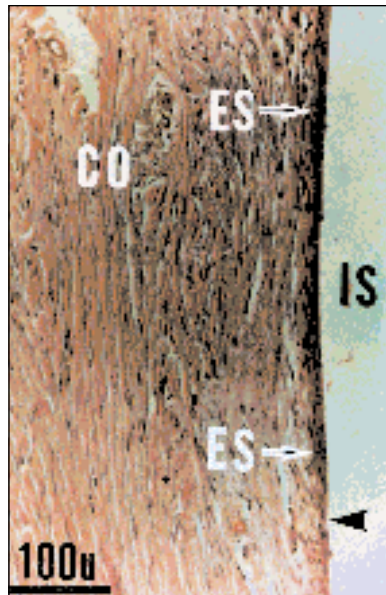
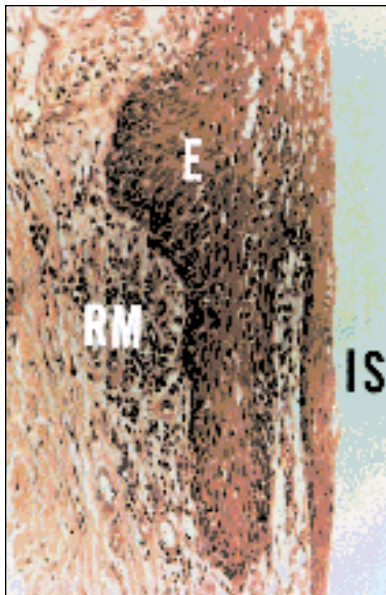


**Fig 4** (Left) Unfavorable implant 36 weeks postimplantation. E = epithelium; RM = round cell migration; IS = implant space.

**Fig 5** (Right) Apical epithelialization continues from Fig 4. IS = implant space; CO = connective tissue; ES = epithelial sheath; *arrowhead* = cervical epithelialization at 8 mm probing depth.

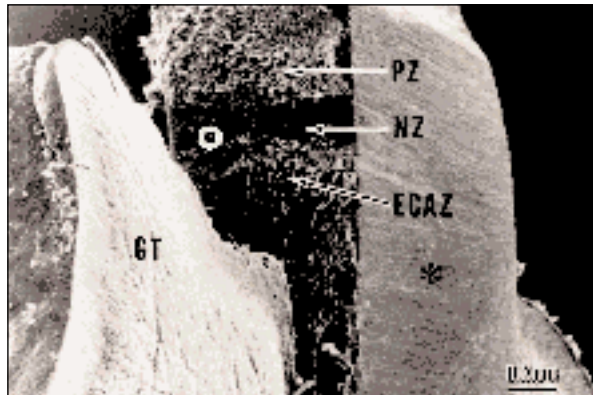


**Fig 6** SEM of abutment post after removal of gingival tissue. GT = gingival tissue; PZ = plaque zone; NZ = nude zone; ECAZ = epithelial cell attachment zone; *asterisk* = cut surface. (White circle indicates the area enlarged in Fig 9a.)

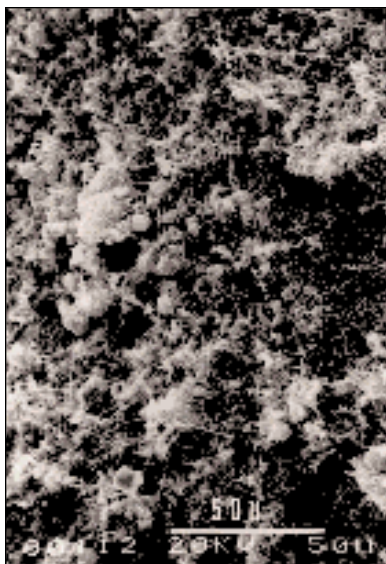


**Fig 7a**

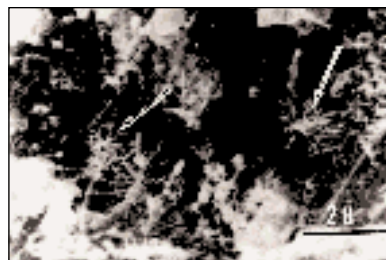


**Fig 7b**

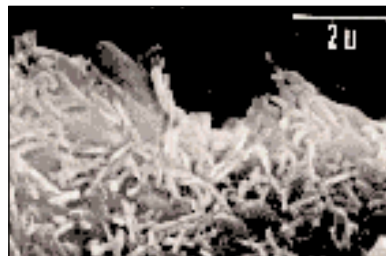


**Fig 7c**

**Fig 7a** SEM of plaque zone showing micrococci in a fine filamentous network.

**Fig 7b** Spirochete colony (*arrows*) in the deep area of PZ.

**Fig 7c** Bacillus colony in the shallow area of PZ.

ment zone (ECAZ) was located in the deepest area of the implant/epithelial tissue interface.

In the PZ, many kinds of microorganisms, such as bacillus, micrococcus, and fine filamentous network (produced by hyphae of yeast), were commonly observed. In addition, a spirochete colony was occasionally observed. The habitats of these colonies were ecologically segregated (Figs 7a to 7c). At the bottom of the implant crevice, a mucous substance was observed in the NZ. The mucous substance consisted of mucin from the saliva and extracellular exudate from the epithelial cells. In addition, some bacterial and/or cellular debris, which were rarely detected by the SEM, were also observed in the NZ (Fig 8). The ECAZ was located at the deepest area of the epithelial cell layer, with the monolayer cell sheet of epithelium strongly attached directly to the implant post surface. Separating the gingival tissue from the implant post did not cause the epithelial cell sheet to detach from the post surface. The attached epithelial cells represented an active living state of microvilli, pseudopodia, and filopodia. Migration of leucocytes was also observed in the intercellular spaces.

In the area of loose cell adhesion at the cell-implant interface, part of the attached epithelial cell sheet was removed from the post surface after the separation (Figs 9a and 9b). An example of the bacterial attack through the mucous area of the NZ to the attached epithelial cell sheet was visible at the NZ-ECAZ interface. The protective biologic mechanism against such an attack was demonstrated by the migration of leucocytes through the intercellular space of the epithelium (Fig 9c).

An SEM micrograph of an unsuccessful implant is shown in Fig 10a. Epithelialization of the unsuccessful implant is exhibited by vigorous elongation of the apical epithelialization along the post surfaces. The epithelial tissue substratum was separated into two layers. One layer was the attached epithelium (AE) to the implant surface; the other layer was the main epithelium (ME) attached to the underlining connective tissue. The separation at the implant-tissue interface may have been caused by thermal shrinkage of the tissue during the freezing process and/or chemical shrinkage during the glutaraldehyde fixation. At a higher magnification (Fig 10b), small gaps between the attached AE and the implant surface and large spaces between the layers of AE and ME were observed. The AE layer was occasionally removed from the implant surface because of the poor adhesive strength at the cell-implant interface (Fig 10b).

**Apical Epithelialization.** In rejecting the implant as a foreign body, epithelialization occurs naturally along the dental implant surface. Protection against apical epithelialization is necessary for retention of



**Fig 8** SEM of the nude zone. The upper white line indicates the border between the PZ and the NZ, and the lower white line indicates the border between the NZ and the ECAZ.

the dental implant. It is known that physicochemical irritation caused by bacterial invasion, food debris ingress, and mechanical movement of the implant promotes epithelialization. In the serviceable implant, epithelialization was prevented at the shallow area of implant-tissue interface by a barrier of connective tissue attachment/adhesion. However, in the case of the unserviceable implant, epithelialization was prevented at the deep area (Fig 10a) of the implant-tissue interface. In addition, the Gingival Indices of the unserviceable implant were higher than were those for the serviceable implants (Table 1).

## Discussion

This study demonstrated the morphologic protocol of the biologic seal that acts as a barrier against bacterial invasion and food debris ingress into the implant-tissue interface.<sup>7</sup> Before discussing the biologic seal, the terminology for tissue/cell attachment or adhesion must be addressed to clear up misunderstandings and to avoid further confusion. For example, "tissue attachment" has been referred to as fibrous tissue intrusion into the dentin and/or cementum of the natural tooth. There is no tissue attachment system for dental implants, except in a very rare case as reported by Buser et al<sup>8</sup> and by Nishihara.<sup>9</sup> Thus, a new technical terminology for dental implantology should be considered.

Based on this report and on previous *in vitro*,<sup>10-14</sup> *in vivo*,<sup>15-20</sup> and clinical investigations<sup>21-25</sup> on the

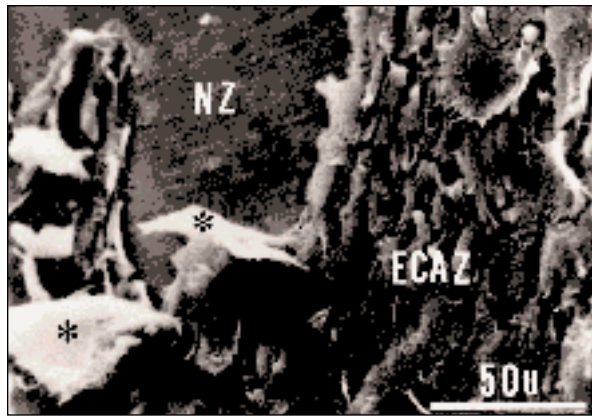


**Fig 9a** Enlarged magnification of the white circle found in the nude zone in Fig 6. Asterisk = cell sheet flap removed from the implant surface.



**Fig 9b** (Left) Enlarged magnification of the upper right corner of Fig 9a showing the presence of a leucocyte (arrow) in the intercellular space.

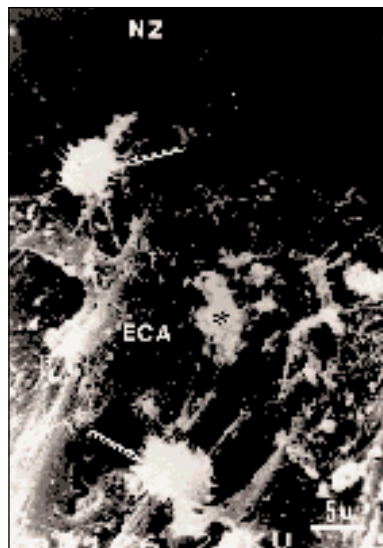


**Fig 9c** (Right) Enlarged magnification of the NZ/ECAZ border in Fig 8 showing the presence of leucocytes (arrow) in the intercellular space and epithelial cells (ECA) on the titanium surface.

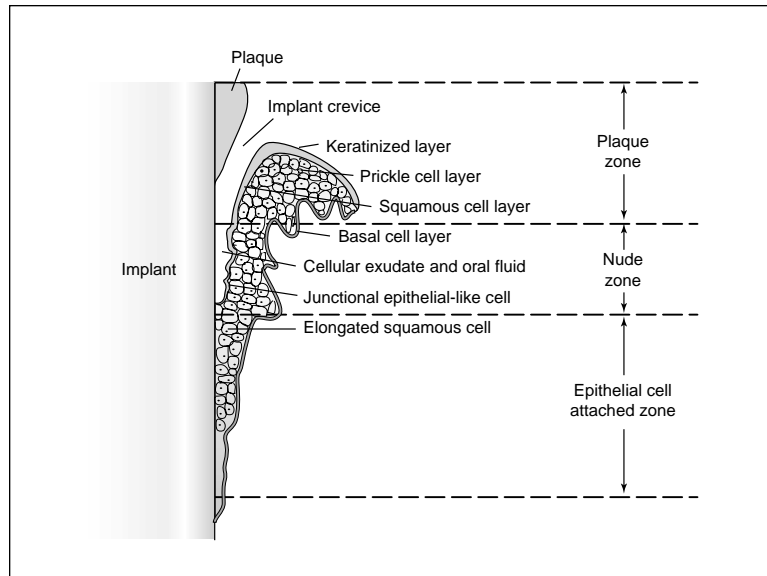


**Fig 10a** (Left) Tissue-implant interface of unfavorable implant. ME = main epithelium; AE = attached epithelium to titanium surface; CT = connective tissue; B = bone. Detached epithelium from the implant surface is indicated by double arrows and the forefront of apical epithelialization is indicated by an arrowhead.



**Fig 10b** (Right) Enlarged magnification of the upper right corner of Fig 10a showing the main epithelium (ME), attached epithelium (AE), epithelial tissue bridge caused by the separation of epithelium (arrows), and the removed flap of epithelial cell sheet (asterisk).

**Fig 11** Schematic drawing showing the three different zones in the biologic seal.



interfacial reaction between the tissue/cell and implant post, it is suggested that the following terms may be appropriate.

The term "cell/tissue attachment to implant" refers to cell/tissue that has direct contact with the implant surface and an interfacial space of basal lamina less than about 200 nm thickness (including hemidesmosome, focal contact,<sup>10,11</sup> and interfacial fusion).<sup>12,19,20</sup> The term "cell/tissue adhesion to implant" indicates an indirect contact or a sandwich layer of glue<sup>19</sup> (about 200 nm or more) between the cell/tissue and implant surfaces. The sandwich layer of glue is composed of an extracellular matrix (exudate) and body/oral fluids. The gingival epithelium may produce a greater bonding strength to the titanium implant surface than that of cell-cell attachment. This was apparent when the epithelial cell sheet remained on the implant surface after the gingival tissue was separated from it (Figs 9a and 10b).

Based on the SEM analyses of PZ, NZ, and ECAZ in Figs 8 and 9c, the role of each zone in the biologic seal may be seen in Fig 11:

1. *Plaque zone*, located at the shallow area of the implant crevice, is the site for buildup of bacteria that can attack the gingival tissue. Quirynen et al<sup>26</sup> and Wu-Yuan et al<sup>27</sup> reported that rough surfaces accumulate up to 25 times more subgingival plaque than smooth surfaces. Implants with a surface roughness of less than 0.2  $\mu\text{m}$  have no major effect on the microbiologic composition subgingivally or supragingivally.<sup>28</sup> Abutment posts with mirror-like surfaces ( $R_z$  value less than 0.5  $\mu\text{m}$ ) demonstrated low bacterial compaction. Espe-

cially in the deep area of the implant crevice, bacterial adhesion together with the soft tissue may be removed by separating the gingival tissue from the post abutment, which may be closely related to formation of the NZ.

2. *Nude zone* is formed by disturbing the epithelial cell attachment/adhesion with bacterial lipopolysaccharides, which have a high affinity for titanium surfaces and severe cytotoxicity.<sup>29</sup> The post surface may be covered with glue-like mucous materials consisting of mucin from saliva, glycoproteins, and laminin. These mucous materials are exuded by the epithelial tissues onto the epithelial tissue-implant interface. The epithelial cells contact the implant surface indirectly through a mucous layer of 200 nm or more thickness. It is suggested that this zone may play a defending role against the physicochemical attack of bacteria and food debris ingress.
3. *Epithelial cell attached zone* occurs at the epithelial tissue-implant interface. It is less than 200 nm thick and has a basal lamina with focal contacts, hemidesmosomes, and/or interfacial fusion.

Two hypotheses on the biologic seal have been discussed during the last 10 years. The first, involving epithelial cell attachment/adhesion to the implant surface, has been supported with histologic research by ten Cate,<sup>15</sup> McKinney et al,<sup>7</sup> Steflick et al,<sup>16</sup> Warrer et al,<sup>18</sup> Kawahara,<sup>19</sup> and Kawahara et al.<sup>20</sup> The other hypothesis was related to a tight band of keratinized epithelium and circular collagen fibers without any epithelial cell attachment. This hypothesis was supported with clinical investigations by Meffert,<sup>21,22</sup>

Ruggeri,<sup>17</sup> Wennstrom et al,<sup>24</sup> and Kirisch.<sup>25</sup> From the SEM and histologic investigations in this study, it is suggested that there are two methods of direct contact with the epithelial cell attachment to the implant surface at the ECAZ and indirect contact with epithelium cell adhesion through the mucous substance of glue at the NZ (Fig 11).

Histologically, the peri-implant gingival tissue was similar to that of the natural tooth with some differences. For the titanium implant, keratinized epithelium was seen to develop toward the implant apex. At the implant crevice, the keratinized epithelium changes its characteristics to a more nonkeratinized condition and transformed to a junctional epithelial-like cell (JELC) at the NZ. If the JELC continues in a normal state, direct contact of cell attachment to the implant surface may be observed by syneresis of the sandwich layer.<sup>19</sup> The JELCs were lined with a squamous cell layer, which was in direct contact with the implant surface at the deep area, and apical epithelialization along the implant surface was prevented with close attachment of a barrier of connective tissues.<sup>30</sup>

In the case of an unserviceable implant, pathologic responses were induced and promoted primarily by the physicochemical irritation of setting cement and secondarily by the presence of cytotoxic elements from plaque and food debris. Degeneration to swelling and karyorrhexis in the keratinized and squamous cell layer, and inflammatory responses with lymphocytic infiltration were observed in the basal and prickle cell layer. Active epithelialization developed toward the apex along the implant surface. At the forefront of epithelialization, the advanced epithelial cells encountered the connective tissues, where both the epithelial and fibroblastic cells competed for adhesion/attachment.

As observed from the SEM analyses (Figs 10a and 10b), the large space in the epithelium was possibly the result of tissue shrinkage from chemical fixation and freezing during SEM specimen preparation. Separation of the epithelial tissue into two layers was also observed. The AE layer was attached to the implant surface and the ME layer was bonded to the connective tissue (CT) layer (Fig 10b). Such findings suggested that the epithelial cell attachment/adhesion to the implant surface has a greater bond strength than the cell-cell bonding within the epithelial tissue layer. As shown in Fig 10b, removal of the AE layer was possible at the poorly adhered portion of the cell-implant interface. From these SEM investigations, it is possible to understand the true state of epithelial attachment/adhesion and apical epithelialization. Active multiplication of epithelial cell developed toward the implant apex and was arrested at the front (Fig 10a) in the area where competition for

adhesion between the epithelial cells and connective tissues occurred.

As for the rise and fall of Gingival Indices during the animal study, the increase in PI from 12 weeks postimplantation (prior to the mounting of the metallic crown) to 24 weeks (12 weeks after the mounting of the metallic crown) was possibly caused by poor self-hygiene. The decrease in PD and PV from 12 weeks to 24 weeks was possibly caused by the mounted crown protecting the implant crevice and surrounding soft tissue from the traumatic presence of hard food debris during functional mastication. In this study, there was no relationship between each Gingival Index. Furthermore, the morphologic observations in the light and SEM investigations (degree of apical epithelialization, depth of implant crevice, width of epithelial cell attachment/adhesion, and inflammatory reactions) did not always agree with the Gingival Indices among the five serviceable implants. However, it must be noted that distinct differences between the Gingival Indices of the five serviceable implants (Table 1) and the unserviceable implant were observed, and these differences were confirmed by the light and SEM investigations. It was also revealed that the upper limits of Gingival Indices for serviceable implants were in the vicinity of 3 mm for PD, 30% for BI, 7 for PV, 3 for MV, and 80% for PI. However, taking into account individual differences between each animal, these Gingival Index data should be reevaluated with a larger sample size in future studies.

## Conclusion

Clinical measurements of Gingival Indices and morphologic observations using light and SEM investigations were performed to verify the defending mechanism of gingival soft tissue against the attack of foreign invasions from the standpoint of epithelial cell adhesion/attachment to the abutment post in vivo. Six commercially pure titanium implants were placed in three monkey mandibles. The following zones were observed using SEM analyses: (1) plaque zone; (2) nude zone; and (3) epithelial cell attached zone at the epithelial tissue-implant post interface. Large concentrations of bacterial organisms were observed in the PZ, suggesting susceptibility of the gingival tissues to bacterial invasion. In the NZ, indirect adhesion of epithelial cells to the implant surface through a mucous layer was observed, and this zone may play a role in defending against physicochemical irritation as a result of bacterial invasion and food debris ingress. Direct attachment of epithelial cells to the implant surface was observed in the ECAZ. A stronger bond strength at the cell-implant interface

was indicated when compared to the cell-cell bonding within the epithelial cell layer.

For the serviceable implants, no significant relationship was observed between the morphologic observations and each Gingival Index. However, distinct differences in the Gingival Indices and morphologic observations were observed between serviceable and unserviceable implants. Gingival Index measurements for serviceable implants indicated an upper limit of 5 mm for the probing depth, 30% for the Bleeding Index, 80% for the Plaque Index, 11 for the Periotron value, and 3 for the mobility value (the mobility value for a normal tooth is 0.5 to 2.5). This study suggests that the epithelial cell attachment/adhesion may play a dominant role in maintaining dental implant integrity.

### Acknowledgments

Financial support for this study was provided by a grant from the Training Institute of the Japanese Society of Oral Implantology (JSOI). The authors would like to thank K. Hashimoto, DDS, PhD, and Ms Y. Ohta for their helpful suggestions and assistance in the study.

### References

- Kawahara H, Tanaka K, Ashiura Y [inventors]. Endosseous implant having polycapillary structure. US patent 4,964,801. 1990.
- Mimura Y, Kawahara H, Hashimoto K. Geometric change of titanium surface by pickling with hydrofluoric acid solution. *Jap J Dent Mater* 1991;10:21–22.
- Kawahara D, Kimura Y, Nakamura M, Kawahara H. Studies on the tissue adhesive capability to titanium by dynamic wettability test and cell attachment, in vitro. *Clin Mater* 1993;14:229–233.
- Hunter F. Periodontal probes and probing. *Int Dent J* 1994;44:577–583.
- Yamagami A, Nishio Y. Relationship between Periotron value and probing depth. In: Kawahara H (ed). *Porous Implant*. Tokyo: Ishiyaku, 1989:110–111.
- Mimura Y, Iwao T, Hashimoto K, Shinkawa I, Kawahara H. A new measuring apparatus for mobility of tooth and implant. *Dent Mater Forum* 1992;5:73–77.
- McKinney RV, Steflik DE, Koth DL. The biological response to the single crystal sapphire endosteal dental implant. *Scanning electron microscopic observations*. *J Prosthet Dent* 1984;51:372–379.
- Buser D, Warrer K, Karring T. Formation of a periodontal ligament around titanium implants. *J Periodontol* 1990;61:597–601.
- Nishihara K. Studies on periodontal tissues around a new type hydroxyapatite artificial root. In: Hulbert JE, Hulbert SF (eds). *Bioceramics*, vol 3. Terre Haute, Indiana: Rose-Hulman Institute of Technology, 1990:171–181.
- Jansen JA. *Epithelial Cell Adhesion to Dental Implant Materials*. The Netherlands: Krips Repro Mepel, Nijmegen, 1984.
- Jansen JA, de Wijn JR, Wolters-Lutgerhorst JML. Ultrastructural study of epithelial cell attachment to implant materials. *J Dent Res* 1985;64:891–896.
- Kawahara H. Cellular responses to implant materials: Biological, physical and chemical factors. *Int Dent J* 1983;33:350–375.
- Burridge K, Fath K, Kelly T, Nucholls G, Turner C. Focal adhesion: Transmembrane junctions between the extracellular matrix and the cytoskeleton. *Ann Rev Cell Biol* 1988;4:487–525.
- Cochran D, Simpson J, Weber HP, Buser D. Attachment and growth of periodontal cells on smooth and rough titanium. *Int J Oral Maxillofac Implants* 1994;9:289–297.
- Ten Cate AR. The gingival junction. In: Brånemark P-I, Zarb GA, Albrektsson T (eds). *Tissue Integrated Prostheses: Osseointegration in Clinical Dentistry*. Chicago: Quintessence, 1985:145–153.
- Steflik DE, McKinney RV, Parr GR, Sisk AL, Koth DL. What we know about the interface between implants and soft tissues. *Oral Maxillofac Surg Clin North Am* 1991;3:775–793.
- Ruggeri K. Supracrestal circular collagen fiber network around osseointegrated nonsubmerged titanium implants. *Clin Oral Implants Res* 1992;3:169–172.
- Warrer K, Buser D, Lang NP, Karring T. Plaque-induced periimplantitis in the presence or absence of keratinized mucosa. *Clin Oral Implants Res* 1995;6:131–138.
- Kawahara H. Biomaterials for dental implants. In: Wise DL, Trantolo DJ, Altobelli DE, Yaszemski MJ, Gresser JD, Schwartz ER (eds). *Encyclopedic Handbook of Biomaterials and Bioengineering*, vol II. New York: Marcel Dekker, 1995:1469–1524.
- Kawahara H, Hashimoto K, Mimura Y. Experimental studies on the biological seal. Part 1: Histological investigation on epithelialization around the implant post. *J Jap Soc Oral Implantol* 1994;7:123.
- Meffert RM. How to treat the ailing and failing implants. *Implant Dent* 1992;1:25–33.
- Meffert RM. Periodontitis and periimplantitis: One and the same? *J Dent Symp* 1993;1:24–28.
- Silverstein LH, Lefkove MD, Garnick JJ. The use of free gingival soft tissue to improve the implant/soft-tissue interface. *J Oral Implantol* 1994;20:36–40.
- Wennstrom JL, Bengazi F, Lekholm U. The influence of the masticatory mucosa on the peri-implant soft tissue condition. *Clin Oral Implants Res* 1994;5:1–8.
- Kirsch A. The intramobile cylinder (IMZ) two-stage osseointegrated implant system with the intramobile element (IME): Short and long term clinical data. *Practical Periodontics Aesthet Dent* 1991;2:24–32.
- Quirynen M, van der Mei HC, Bollen CM, Schotte A, Marechal M, Doornbusch GI, et al. An in vivo study of the influence of the surface roughness of implants on the microbiology of supra- and subgingival plaque. *J Dent Res* 1993;72:1304–1309.
- Wu-Yuan CD, Eganhouse KJ, Keller JC, Walters KS. Oral bacterial attachment to titanium surfaces: A scanning electron microscopy study. *J Oral Implantol* 1995;21:207–213.
- Quirynen M, Bollen CM, Papaioannou W, van Eldere J, van Steenberghe D. The influence of titanium abutment surface roughness on plaque accumulation and gingivitis: Short-term observations. *Int J Oral Maxillofac Implants* 1996;11:169–178.
- Nelson SK, Knoernschild KL, Robinson FG, Schuster GS. Lipopolysaccharide affinity for titanium implant biomaterials. *J Prosthet Dent* 1997;77:76–82.
- Kawahara H, Hashimoto K, Mimura Y, Takashima Y. Experimental study on the biological seal. Part 1: Histopathological investigation on the epithelialization around the implant post. *J Jap Soc Oral Implantol* 1994;7:123–124.